

A New Formulation for the Torsional Vibration Analysis of Rotating Cantilever Rods

Hong H. Yoo,* Christophe Pierre** and Robert R. Ryan***

(Received June 1, 1996)

This paper presents a new modeling method for the analysis of torsional vibration of rotating cantilever rods. The natural frequency and mode shape variations due to the rotational motion could be accurately estimated with the modeling method, and the coefficients for the well-known Southwell equation could be obtained, as well. This method has couple of advantages compared to previous conventional modeling methods. Different from the previous modeling methods, the equations of motion of the rotating cantilever rod were derived with consistent linearization in a rigorous way. An eigenvalue problem to obtain the coefficients of the Southwell equation of rotating rods were derived from the original eigenvalue problem.

Key Words : Torsional Vibration, Rotating Rods, Frequency Variation, Southwell equation

1. Introduction

It is well known that the modal characteristics of rotating structures often vary significantly compared to non-rotating structures. Inertial forces caused by centrifugal motions result in the variations of natural frequencies and mode shapes. The importance of the variations has been recognized in many engineering examples such as rotating blades in turbines, turbomachines, and aircrafts. As modern mechanical systems become increasingly oriented to high-speed, light-weight, and low energy consumption, such variations of modal characteristics become more critical for the system design.

Torsional stiffness variation due to stretching has been a subject of study for many researchers. Earlier pioneering works were performed by Wagner (1936) and Biot (1939). Wagner examined the general mechanism of the effect of

longitudinal stresses on torsional rigidity for arbitrary open sections of rods, and explained the resulting increase in torsional stiffness intuitively. Biot applied the theory of elasticity to show the same increase in torsional stiffness. More rigorous works followed by other researchers. Chu (1952), Houbolt and Brooks (1958), and Carnegie (1959) studied the effect of pretwist on torsional stiffness, and Niedenfuhr (1955) included the effects of nonlinear twist and axial tension. Budiansky and Meyers (1956) studied the effect of aerodynamic heating on the effective torsional stiffness of thin wings, and Goodier (1950) investigated the effect of initial axial stress on torsional stiffness. Exact intrinsic equations for moving beams were presented by Borri and Mantegazza (1958) and Hodges (1989), and both references obtained the same exact one-dimensional equations. Borri and Merlini (1986) showed that the constitutive equations could be obtained in an incremental analysis with the stiffening effect due to an axial force stemming from the constitutive law. Even though the stiffening effect was derived in the most general form, they neglected the incremental change in warping. A limited asymptotic approach was also undertaken by Berdichevskii (1981). Shield (1984) and Danielson and Hodges (1987) attempt-

* Associate Professor, Department of Mechanical Design and production Engineering, Hanyang University

** Professor, Department of Mechanical Engineering and Applied Mechanics, The University of Michigan at Ann Arbor

*** Vice President, Mechanical Dynamics, Inc.

ed to obtain correct expressions for the engineering strain, which are valid for any arbitrary deformations, with somewhat disappointing results due to the higher powers of warping gradients contained in the equations. Carnegie (1962), Hodges and Dowell (1974), and Kaza and Kvaternik (1974) studied the increase of torsional stiffness due to warping. Torsional vibrations of rotating rods were studied explicitly by Bogdanoff and Horner (1956), Duggan and Slyper (1969), Kaza and Kielb (1984), and Subrahmanyam and Kaza (1985). All the works mentioned so far led to a standard, or conventional approach for dealing with torsional vibrations. This approach, which is described in the next paragraph provide a context for introducing a new analysis procedure in this paper.

The conventional approach used to obtain the natural frequencies of rotating rods can be summarized as follows. Two nonlinear partial differential equations are derived: one governing stretching and the other governing torsion. From the equation governing stretching, an equation relating the tensile force to the centrifugal inertia force is obtained by neglecting all other terms. Then the relating equation is used for the equation governing torsion. Since the tensile force which was originally of first degree becomes zeroth degree (centrifugal inertia force), a linear equation containing the stretching effect due to rotation can be derived. The basic problem of this approach lies in the assumption that all terms other than the tensile force and the centrifugal force are negligible. Such assumption may or may not be true, in general. For instance, if a coupling exists between the stretching and torsional equations, the assumption leads to inaccurate results as the rotating angular speed increases. The assumption is not necessary for the approach presented in this paper, which is based on a rigorous and consistent linearization. Furthermore, the tedious, complicated, and involved steps required for the conventional procedures are not necessary for the proposed approach.

The purpose of this paper is to present a modeling method for torsional vibration analysis of rotating cantilever rods, by which one can

accurately predict the natural frequencies and mode shapes. As mentioned above, the merit of the method lies in the simplicity, consistency, and rigorousness of the procedure of deriving equations of motion. In this paper, rather than considering all complicated effects (for instance, warping and eccentricity), the central issue is focused on the stiffness variation due to rotation. Kane's method (see Kane and Levinson, 1985) along with the assumed mode method (see Meirovitch, 1980) are utilized to derive the equations of motion without dealing with partial differential equations. This paper also presents a way of calculating the coefficients of Southwell equations for rotating cantilever rods. The coefficients are conveniently used to calculate the torsional natural frequencies of rotating rods.

2. The Strain Energy of a Rod in Torsion and Stretching

The system to be analyzed, shown in Fig. 1, consists of a cantilever rod B built into a rigid body R (rigid hub having radius r) in which a unit vector triad \bar{a}_1 , \bar{a}_2 and \bar{a}_3 is fixed. The rod is characterized by a natural length L , material properties E (Young's modulus), G (shear modulus), ρ (mass per unit length), and A (cross-sectional area). The cross-section of the rod considered in this paper has high thickness ratio (defined by the value of the smallest dimension divided by the largest dimension of the cross-section). Let x be a distance from a point O , located on the elastic axis of the rod at the intersection of B and R , to the shear center P of a

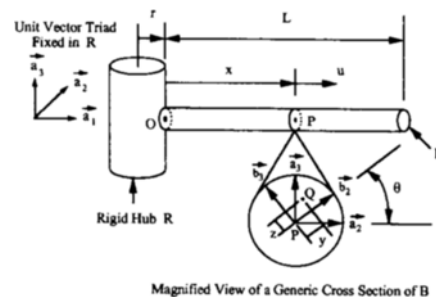


Fig. 1 Deformation of a rod with a uniform cross section

generic cross-section of B in the undeformed state. The generic cross-section is assumed to be rigid (i. e. no warping occurs), and rotates around the elastic axis of the rod. In the rigid cross-section, another unit vector triad \vec{b}_1 , \vec{b}_2 , and \vec{b}_3 , is fixed. In the undeformed state of the rod, the unit vector triad of the rigid cross-section coincides with that of the rigid body R . The unit vectors of the rigid cross-section change their directions as deformation occurs. Only the deformation of stretching, denoted by u , and that of torsion, denoted by θ , are considered. The deformation due to warping is not considered here. After stretching occurs, the distance between the point O and the point P becomes $x + u$. However, the stretching does not alter the orientation of the unit vectors fixed in the rigid cross-section of the rod. Only torsional movements change the orientation of some of these unit vectors. The unit vectors fixed in B can be related to the unit vectors fixed in A as follows:

$$\vec{b}_1 = \vec{a}_1 \quad (1)$$

$$\vec{b}_2 = \cos\theta \vec{a}_2 + \sin\theta \vec{a}_3 \quad (2)$$

$$\vec{b}_3 = -\sin\theta \vec{a}_2 + \cos\theta \vec{a}_3 \quad (3)$$

where θ is a rotational angle of the rigid cross section.

Two variables, y and z , represent the projection of the distance from the point P to an arbitrary point Q of the cross-section along directions \vec{b}_2 and \vec{b}_3 .

One needs to derive expressions of the strains in order to obtain the strain energy of the rod. For that purpose, Green's strain measures will be derived. The engineering strain measures, as well as their approximate expressions up to the second degree in the deformation variables, will then be formulated from the expressions of Green's strain measures. Contrary to Green's strains, which require the corresponding second Piola Kirchhoff stresses to obtain the strain energy of the rod, engineering strains provide a direct way of obtaining the strain energy expression. Moreover, since *linear* equations of motion are to be derived, only the second-degree approximation of the engineering strain measures are necessary. These approximate strain expressions are used to

obtain the strain energy of the rod.

In order to derive Green's strains, the following position vector and its tangent vectors are introduced. The position vector, connecting the points O and Q , is denoted by \vec{p} , and expressed as

$$\vec{p} = (x + u)\vec{b}_1 + y\vec{b}_2 + z\vec{b}_3 \quad (4)$$

The tangent vectors of the position vector are defined as

$$\vec{G}_x \triangleq \frac{\partial \vec{p}}{\partial x} \quad (5)$$

$$\vec{G}_y \triangleq \frac{\partial \vec{p}}{\partial y} \quad (6)$$

$$\vec{G}_z \triangleq \frac{\partial \vec{p}}{\partial z} \quad (7)$$

Therefore, from Eqs. (4), (5), (6) and (7), one obtains

$$\vec{G}_x = \left(1 + \frac{du}{dx}\right)\vec{b}_1 - z\frac{d\theta}{dx}\vec{b}_2 + y\frac{d\theta}{dx}\vec{b}_3 \quad (8)$$

$$\vec{G}_y = \vec{b}_2 \quad (9)$$

$$\vec{G}_z = \vec{b}_3 \quad (10)$$

Note that u and θ are functions of x , but not of y and z . Using \vec{G}_x , \vec{G}_y , and \vec{G}_z , Green's strain measures can be expressed as follows (see Wempner, 1973):

$$\epsilon_{xx} = \frac{1}{2}(\vec{G}_x \cdot \vec{G}_x - 1) \quad (11)$$

$$\epsilon_{yy} = \frac{1}{2}(\vec{G}_y \cdot \vec{G}_y - 1) \quad (12)$$

$$\epsilon_{zz} = \frac{1}{2}(\vec{G}_z \cdot \vec{G}_z - 1) \quad (13)$$

$$\gamma_{xy} = \vec{G}_x \cdot \vec{G}_y \quad (14)$$

$$\gamma_{yz} = \vec{G}_y \cdot \vec{G}_z \quad (15)$$

$$\gamma_{zx} = \vec{G}_z \cdot \vec{G}_x \quad (16)$$

Using Eqs. (8~10), one obtains

$$\epsilon_{xx} = \frac{du}{dx} + \frac{1}{2}\left(\frac{du}{dx}\right)^2 + \frac{1}{2}(y^2 + z^2)\left(\frac{d\theta}{dx}\right)^2 \quad (17)$$

$$\epsilon_{yy} = 0 \quad (18)$$

$$\epsilon_{zz} = 0 \quad (19)$$

$$\gamma_{xy} = -z\frac{d\theta}{dx} \quad (20)$$

$$\gamma_{yz} = 0 \quad (21)$$

$$\gamma_{zx} = y\frac{d\theta}{dx} \quad (22)$$

Note that Eqs. (18), (19) and (21) constitute the conventional assumptions of Euler beam.

If Green's strain measures were used to obtain the strain energy expression of the rod, one would need to derive the second Piola Kirchhoff stress expressions. However, the strain energy can be directly obtained from the engineering strain measures. The engineering strain for stretching, denoted by ϵ , and be expressed as

$$\epsilon = -1 + \sqrt{1 + 2\epsilon_{xx}} \quad (23)$$

Since linear equations of motion of the rod are to be derived, a second-degree approximation of the engineering strain is sufficient. This second-degree approximation of ϵ is often referred to as the von Kármán strain measure of rod, and it will be denoted by ϵ_k . Substituting Eq. (17) into Eq. (23) and retaining terms up to the second-degree of the deformations, ϵ_k is obtained as

$$\epsilon_k = \frac{du}{dx} + \frac{1}{2}(y^2 + z^2)\left(\frac{d\theta}{dx}\right)^2 \quad (24)$$

The strain energy based on the von Kármán strain measure ϵ_k and the shear strains γ_{xy} and γ_{zx} is give by

$$U = U_1 + U_2 \quad (25)$$

where

$$U_1 = \frac{1}{2} \int_0^L \int_S E \epsilon_k^2 dA dx \quad (26)$$

$$U_2 = \frac{1}{2} \int_0^L \int_S G (\gamma_{xy}^2 + \gamma_{zx}^2) dA dx \quad (27)$$

where S represents the domain of the cross section of the rod. Substituting the expressions of ϵ_k , γ_{xy} , and γ_{zx} into Eqs. (26) and (27) yields

$$U_1 = \frac{1}{2} \int_0^L \int_S E \left[\frac{du}{dx} + \frac{1}{2}(y^2 + z^2)\left(\frac{d\theta}{dx}\right)^2 \right]^2 dA dx \quad (28)$$

$$U_2 = \frac{1}{2} \int_0^L \int_S G (y^2 + z^2)\left(\frac{d\theta}{dx}\right)^2 dA dx \quad (29)$$

Taking advantage of the fact that u and θ are independent from y and z , Eq. (28) can be restated as

$$U_1 = \frac{1}{2} \int_0^L EA \left(\frac{du}{dx}\right)^2 dx + \frac{1}{2} \int_0^L EJ \left(\frac{du}{dx}\right)\left(\frac{d\theta}{dx}\right)^2 dx + \frac{1}{8} \int_0^L EJ_2 \left(\frac{d\theta}{dx}\right)^4 dx \quad (30)$$

where

$$J \triangleq \int_S (y^2 + z^2) dA \quad (31)$$

$$J_2 \triangleq \int_S (y^2 + z^2)^2 dA \quad (32)$$

Now, let's define a variables as

$$s \triangleq u + \frac{1}{2} \int_0^x \alpha \left(\frac{d\theta}{d\sigma}\right)^2 d\sigma \quad (33)$$

Where α represents a ratio of J/A . By using the new variable, Eq. (25) can be transformed into the following form

$$U = \frac{1}{2} \int_0^L EA \left(\frac{ds}{dx}\right)^2 dx + \frac{1}{2} \int_0^L GJ \left(\frac{d\theta}{dx}\right)^2 dx \quad (34)$$

To be rigorous, the strain energy expression in Eq. (34), is not exactly equivalent to that given by Eq. (25). However, the difference between these two strain energy expressions is the fourth degree integral terms, which are very small compared with the other terms. These fourth-degree terms, of course, do not affect the linear equations of motion. Therefore, the strain energy expression of Eq. (34) is accurate enough to replace the original form of Eq. (25) for the present context.

In this section, a quadratic form for the strain energy of the rod was derived as Eq. (34). This strain energy expression will be used to derive the equations of motion in the next section. Since the new variable, s , is used for the strain energy, it will also be included in the inertial terms in the equations of motion. The use of the variable, s , is one of the key differences between the proposed and the conventional methods of deriving the equations of motion, as the latter uses only Cartesian deformation variables (e. g., u).

3. Equations of Motion

If the motion of the rigid base R in Fig. 1 is prescribed by a constant angular velocity $\tilde{\omega}^R$, equal to $\Omega \tilde{a}_3$, without translational motion, the kinematic expressions of the velocity and acceleration of point P can be expressed as

$$\tilde{v}^P = \dot{u} \tilde{a}_1 + \Omega(r + x + u) \tilde{a}_2 \quad (35)$$

$$\tilde{a}^P = [\ddot{u} - \Omega^2(r + x + u)] \tilde{a}_1 + 2\Omega \dot{u} \tilde{a}_2 \quad (36)$$

where a dot over a symbol means time differentiation, and a double dot means double time differentiation. Eccentricity effects (discrepancy between elastic and centroidal axes) are not considered in this paper; thus, the expressions in Eqs. (35) and (36) can be used to obtain the inertia force terms in the equations of motion of the rod. The angular velocity and angular acceleration of the rigid cross section of the rod B are

$$\dot{\omega}^B = \dot{\theta} \tilde{a}_1 + \Omega \tilde{a}_3 \quad (37)$$

$$\ddot{\alpha}^B = \ddot{\theta} \tilde{a}_1 + \Omega \dot{\theta} \tilde{a}_3 \quad (38)$$

These can be used to obtain the rotatory inertia terms (related to the rigid body motion of the cross section of the rod) in the equations of motion.

As discussed in the previous section, the variable s defined in Eq. (33) will be used to derive the equations of motion. Therefore, in Eqs. (35) and (36), u , \dot{u} , and \ddot{u} should be replaced by the following expressions.

$$u = s - \frac{1}{2} \int_0^x \alpha \left(\frac{d\theta}{d\sigma} \right)^2 d\sigma \quad (39)$$

$$\dot{u} = \dot{s} - \int_0^x \alpha \left(\frac{d\theta}{d\sigma} \right) \left(\frac{d\dot{\theta}}{d\sigma} \right) d\sigma \quad (40)$$

$$\ddot{u} = \ddot{s} - \int_0^x \alpha \left[\left(\frac{d\theta}{d\sigma} \right) \left(\frac{d\ddot{\theta}}{d\sigma} \right) + \left(\frac{d\dot{\theta}}{d\sigma} \right)^2 \right] d\sigma \quad (41)$$

Then, Eqs. (35) and (36) are transformed as

$$\begin{aligned} \tilde{v}^P = & \left[\dot{s} - \int_0^x \alpha \left(\frac{d\theta}{d\sigma} \right) \left(\frac{d\dot{\theta}}{d\sigma} \right) d\sigma \right] \tilde{a}_1 \\ & + \Omega \left[r + x + s - \frac{1}{2} \int_0^x \alpha \left(\frac{d\theta}{d\sigma} \right)^2 d\sigma \right] \tilde{a}_2 \end{aligned} \quad (42)$$

$$\begin{aligned} \tilde{a}^P = & \left\{ \dot{s} - \int_0^x \alpha \left[\left(\frac{d\theta}{d\sigma} \right) \left(\frac{d\ddot{\theta}}{d\sigma} \right) + \left(\frac{d\dot{\theta}}{d\sigma} \right)^2 \right] d\sigma \right. \\ & \left. - \Omega^2 \left[r + x + s - \frac{1}{2} \int_0^x \alpha \left(\frac{d\theta}{d\sigma} \right)^2 \right] \right\} \tilde{a}_1 \\ & + 2\Omega \left[\dot{s} - \int_0^x \alpha \left(\frac{d\theta}{d\sigma} \right) \left(\frac{d\dot{\theta}}{d\sigma} \right) d\sigma \right] \tilde{a}_2 \end{aligned} \quad (43)$$

Now, by using the assumed mode method, the continuous variables $s(x, t)$ and $\theta(x, t)$ are represented as

$$s(x, t) = \sum_{j=1}^{\mu} \Phi_{1j}(x) q_j(t) \quad (44)$$

$$\theta(x, t) = \sum_{j=1}^{\mu} \Phi_{2j}(x) q_j(t) \quad (45)$$

where

$$\begin{aligned} \Phi_{1j} &= 0 \quad \text{if } \mu_1 + 1 \leq j \leq \mu_1 + \mu_2 \\ \Phi_{2j} &= 0 \quad \text{if } 1 \leq j \leq \mu_1 \end{aligned} \quad (46)$$

and Φ_{1j} , Φ_{2j} ($j=1, \dots, \mu$) are assumed spatial functions, q_j ($j=1, \dots, \mu$) are generalized coordinates, μ_1 and μ_2 are the numbers of spatial functions representing s and θ , respectively, and μ is the total number of modal terms in the series (*i. e.*, $\mu = \mu_1 + \mu_2$). With this discretization, ordinary differential equations of motion can be developed using the following equation (see Kane and Levinson, 1985) if no external force is considered.

$$\begin{aligned} \int_0^L \rho \left(\frac{\partial \tilde{v}^P}{\partial \dot{q}_i} \right) \cdot \tilde{a}^P dx + \int_0^L \rho \frac{\partial \tilde{\omega}^B}{\partial \dot{q}_i} \cdot \\ (\tilde{a}^B \cdot \mathbf{I} + \tilde{\omega}^B \times \mathbf{I} \cdot \tilde{\omega}^B) dx + \frac{\partial U}{\partial q_i} = 0 \\ (i=1, \dots, \mu) \end{aligned} \quad (47)$$

where $\rho \mathbf{I}$ represents the central inertia dyadic per unit length of the rod. The partial derivative of the velocity of point P with respect to the generalized speed \dot{q}_i is

$$\begin{aligned} \frac{\partial \tilde{v}^P}{\partial \dot{q}_i} = & \left[\Phi_{1i} - \sum_{j=1}^{\mu} \left(\int_0^x \alpha \Phi_{2i,\sigma} \Phi_{2j,\sigma} d\sigma \right) q_j \right] \tilde{a}_1 \\ (i=1, \dots, \mu) \end{aligned} \quad (48)$$

and the partial derivative of $\tilde{\omega}^B$ with respect to \dot{q}_i is expressed as.

$$\frac{\partial \tilde{\omega}^B}{\partial \dot{q}_i} = \Phi_{2i} \tilde{a}_1 \quad (i=1, \dots, \mu) \quad (49)$$

The terms $\Phi_{2i,\sigma}$ and $\Phi_{2j,\sigma}$ in Eq. (48) denote spatial differentiation of $\Phi_{2i,\sigma}$ and Φ_{2j} with respect to the dummy variable σ representing x . The Eqs. (48) and (49), along with the expressions for the system strain energy and the acceleration of point P , are used in Eq. (47) to derive the equations of motion.

Ignoring all the nonlinear terms (in terms of the q_i 's), a set of linear equations of motion is obtained as

$$\begin{aligned} \sum_{j=1}^{\mu_1} \left[\int_0^L \rho \phi_{1i} \phi_{1j} dx \ddot{q}_{1j} - \Omega^2 \int_0^L \rho \phi_{1i} \phi_{1j} dx q_{1j} \right. \\ \left. + \int_0^L EA \phi_{1i,x} \phi_{1j,x} dx q_{1j} \right] \\ = \Omega^2 \int_0^L \rho x \phi_{1i} dx + r \Omega^2 \int_0^L \rho \phi_{1i} dx \\ (i=1, 2, \dots, \mu_1) \end{aligned} \quad (50)$$

$$\sum_{j=1}^{\mu_2} \left[\int_0^L \rho \alpha \phi_{2i} \phi_{2j} dx \ddot{q}_{2j} + \int_0^L GJ \phi_{2i,x} \phi_{2j,x} dx q_{2j} \right]$$

$$\begin{aligned} & + \left(r\Omega^2 \int_0^L \rho(L-x)\alpha\phi_{2i,x}\phi_{2j,x}dx \ q_{2j} \right. \\ & \left. + \Omega^2 \int_0^L \frac{\rho}{2}(L^2-x^2)\alpha\phi_{2i,x}\phi_{2j,x}dx \ q_{2j} \right) = 0 \\ & (i=1, 2, \dots, \mu_2) \end{aligned} \quad (51)$$

where $\rho\alpha$ denotes the first component of the central principal inertia dyadic of the rod. It should be noted that the component notations, q_{1i} and q_{2i} , are used instead of q_i in Eqs. (50) and (51); similarly ϕ_{1i} and ϕ_{2i} are used instead of ϕ_i and ϕ_{2i} . The following relations hold for these component notations.

$$\begin{aligned} q_{1i} &= q_i \quad (1 \leq i \leq \mu_1) \\ q_{2i} &= q_{(i+\mu_1)} \quad (1 \leq i \leq \mu_2) \end{aligned} \quad (52)$$

$$\begin{aligned} \phi_{1i} &= \Phi_{1i} \quad (1 \leq i \leq \mu_1) \\ \phi_{2i} &= \Phi_{2(i+\mu_1)} \quad (1 \leq i \leq \mu_2) \end{aligned} \quad (53)$$

Equations (50) and (51) show that the two sets of equations are completely decoupled; yet, the torsional stiffness variation due to rotation is clearly present in Eq. (51). In the next section, Eq. (51) is transformed into a non-dimensional form which will be used to obtain the natural frequencies and mode shapes of rotating cantilever rods.

4. Modal Analysis Formulation

In Sec. 3, a set of linear equations governing torsion of rotating cantilever rods was obtained in Eq. (51). The torsional equation set, however, involves several parameters and variables (*e. g.* ρ , L , G , J , α , Ω , t , and x), and it is useful to rewrite it in a non-dimensional form. To achieve this, the following non-dimensional variables are introduced.

$$\tau \triangleq \frac{t}{T} \quad (54)$$

$$\chi \triangleq \frac{x}{L} \quad (55)$$

$$\vartheta_j \triangleq \frac{q_{2j}}{L} \quad (56)$$

$$T = \frac{2L}{\pi} \left(\frac{\rho}{GA} \right)^{\frac{1}{2}} \quad (57)$$

Introducing these non-dimensional variables into Eq. (51), one obtains:

$$\begin{aligned} & \sum_{j=1}^{\mu_2} \left[\int_0^1 \psi_{2i}\psi_{2j}d\chi \vartheta_j + \frac{4}{\pi^2} \int_0^1 \psi_{2i,x}\psi_{2j,x}d\chi \vartheta_j \right. \\ & \left. + \delta\gamma^2 \int_0^1 (1-\chi)\psi_{2i,x}\psi_{2j,x}d\chi \vartheta_j \right. \\ & \left. + \frac{1}{2}\gamma^2 \int_0^1 (1-\chi^2)\psi_{2i,x}\psi_{2j,x}d\chi \vartheta_j \right] = 0 \\ & (i=1, 2, \dots, \mu_2) \end{aligned} \quad (58)$$

where $\psi(\chi)$ is equal to $\phi(x)$, and a dot over a symbol now means differentiation with respect to τ . Also there appear new non-dimensional parameters defined as

$$\delta \triangleq \frac{r}{L} \quad (59)$$

$$\gamma \triangleq \Omega T \quad (60)$$

where δ , defined in Eq. (59), is often called the hub radius ratio, and γ , defined in Eq. (60), represents the ratio of the angular speed of the rotating rod to the fundamental natural torsional frequency of the non-rotating rod. Note that the cross section variable α disappeared in Eq. (58). Unless the warping effect is considered, the shape of the cross section does not affect the modal characteristics of the rotating rod. The focus in the next section lies on the effects of two non-dimensional parameters, δ and γ , on the natural frequencies and mode shapes of the rotating rod.

From the non-dimensional Eq. (58), the eigenvalue problem for torsional vibrations of rotating cantilever rods can be derived, assuming that ϑ_i s are harmonic functions of τ (dimensionless time). If ϑ represents a column matrix with ϑ_i s as its elements, it can be expressed as

$$\vartheta = e^{j\omega\tau} \xi \quad (61)$$

where ω is the ratio of the torsional natural frequency of the rotating rod to the fundamental torsional natural frequency of the non-rotating rod, and ξ is a constant column matrix characterizing the deflection shape of the synchronous motion. This yields

$$\omega^2 M \xi = K \xi \quad (62)$$

where M and K are square matrices of size $(\mu_2 \times \mu_2)$, whose respective elements M_{ij} and K_{ij} are defined as

$$M_{ij} \triangleq \int_0^1 \psi_{2i}\psi_{2j}d\chi \quad (63)$$

Table 1 Convergence of natural frequencies with increasing number of modes

Number of modes	First frequency	Second frequency	Third frequency
1	16.78144	*****	*****
2	16.00843	44.27073	*****
3	15.89594	40.36260	74.66436
4	15.83029	39.21226	67.37527
5	15.80705	38.55679	64.70778
6	15.78941	38.21811	63.07738
7	15.78107	37.98298	62.12078
8	17.77402	37.83731	61.43141
9	15.77014	37.72639	60.96342
10	15.76667	37.65073	60.59966
11	15.76457	37.58986	60.33315
12	15.76262	37.54573	60.11646
13	15.76136	37.50891	59.94988
14	15.76017	37.48104	59.81027
15	15.75936	37.45716	59.69928
16	15.75858	37.43852	59.60417
17	15.75803	37.42222	59.52665
18	15.75749	37.40918	59.45909
19	15.75710	37.39759	59.40294
20	15.75672	37.38815	59.35334

$$\begin{aligned}
 K_{ij} \triangleq & \frac{4}{\pi^2} \int_0^1 \psi_{2i,\chi} \psi_{2j,\chi} d\chi \\
 & + \delta \gamma^2 \int_0^1 (1-\chi^2) \psi_{2i,\chi} \psi_{2j,\chi} d\chi \\
 & + \frac{1}{2} \gamma^2 \int_0^1 (1-\chi^2) \psi_{2i,\chi} \psi_{2j,\chi} d\chi \quad (64)
 \end{aligned}$$

The eigenfunctions of the non-rotating rod are chosen as assumed modes; thus

$$\begin{aligned}
 \psi_{2i}(\chi) = & \sqrt{2} \sin \left[(2i-1) \frac{\pi}{2} \chi \right] \\
 (i=1, 2, \dots, \mu_2) \quad & (65)
 \end{aligned}$$

These functions satisfy orthogonality conditions which make the mass matrix M the identity matrix.

As the non-dimensional angular speed γ increases the first term of Eq. (64) becomes negligible compared to other two terms. Then Eq. (62) can be written as follows:

$$\lambda M \xi = K^* \xi \quad (66)$$

where λ and K_{ij}^* are defined by

$$\lambda \triangleq \left(\frac{\omega}{\gamma} \right)^2 \quad (67)$$

$$\begin{aligned}
 K_{ij}^* \triangleq & \delta \int_0^1 (1-\chi) \psi_{2i,\chi} \psi_{2j,\chi} d\chi \\
 & + \frac{1}{2} \gamma^2 \int_0^1 (1-\chi^2) \psi_{2i,\chi} \psi_{2j,\chi} d\chi \quad (68)
 \end{aligned}$$

As defined in Eq. (67), λ denotes the square of the asymptotic slope of the eigenvalue loci. Southwell equation is written as follows:

$$\omega_{ni}^2 = \omega_{0i}^2 + S_i \Omega^2 \quad (69)$$

where ω_{ni} and ω_{0i} denote the i-th natural frequency of the rotating and non-rotating structure, respectively, and Ω denotes the rotating frequency. As the angular speed increases, S becomes asymptotically the square of the ratio of the natural frequency to rotating frequency. Thus, it is equivalent to λ in Eq. (67).

5. Numerical Results and Discussions

In order to obtain accurate numerical results, several assumed modes were used to construct the matrices defined in Eqs. (63) and (64). Due to the property of uniform convergence of the solution for linear systems, convergence can be easily

Table 2 Lowest three natural frequencies with different hub radius and angular speeds

Angular speed γ	Hub radius $\delta=0$			Hub radius $\delta=1$			Hub radius $\delta=5$		
	1st Freq	2nd Freq	3rd Freq	1st Freq	2nd Freq	3rd Freq	1st Freq	2nd Freq	3rd Freq
0.01	1.00005	3.00013	5.00021	1.00014	3.00032	5.00052	1.00049	3.00109	5.00177
0.02	1.00021	3.00051	5.00083	1.00056	3.00128	5.00209	1.00195	3.00437	5.00709
0.03	1.00048	3.00115	5.00187	1.00126	3.00289	5.00469	1.00437	3.00982	5.01593
0.04	1.00086	3.00204	5.00333	1.00224	3.00513	5.00833	1.00775	3.01742	5.02825
0.05	1.00134	3.00319	5.00520	1.00350	3.00801	5.01301	1.01208	3.02714	5.04401
0.06	1.00193	3.00459	5.00748	1.00503	3.01152	5.01871	1.01733	3.03894	5.06315
0.07	1.00262	3.00624	5.01018	1.00685	3.01566	5.02544	1.02349	3.05279	5.08560
0.08	1.00343	3.00815	5.01329	1.00893	3.02042	5.03318	1.03054	3.06862	5.11127
0.09	1.00433	3.01030	5.01681	1.01128	3.02582	5.04193	1.03845	3.08639	5.14008
0.10	1.00535	3.01271	5.02074	1.01391	3.03181	5.05168	1.04720	3.10605	5.17193
0.20	1.02119	3.05039	5.08220	1.05425	3.12404	5.20145	1.17446	3.39162	5.63411
0.30	1.04700	3.11172	5.18216	1.11753	3.26858	5.43585	1.35484	3.79575	6.28606
0.40	1.08197	3.19477	5.31737	1.19941	3.45543	5.73833	1.56751	4.27157	7.05074
0.50	1.12514	3.29722	5.48397	1.29579	3.67518	6.09333	1.80010	4.79163	7.88340
0.60	1.17552	3.41670	5.67796	1.40331	3.92013	6.48816	2.04559	5.34062	8.75972
0.70	1.23213	3.55088	5.89548	1.51938	4.18441	6.91319	2.29987	5.90982	9.66642
0.80	1.29410	3.69766	6.13303	1.64205	4.46366	7.36126	2.56041	6.49396	10.59596
0.90	1.36064	3.85519	6.38756	1.76989	4.75469	7.82735	2.82559	7.08969	11.54375
1.00	1.43107	4.02189	6.65646	1.90184	5.05516	8.30774	3.09431	7.69475	12.50675
2.00	2.25908	5.98424	9.80029	3.33580	8.33886	13.54030	5.87367	14.03084	22.63519
3.00	3.18415	8.19283	13.32542	4.85063	11.85229	19.15410	8.71373	20.59440	33.17148
4.00	4.14291	10.50158	17.01677	6.39178	15.46048	24.93079	12.57183	27.23634	43.84776
5.00	5.11711	12.86308	20.80028	7.94471	19.11660	30.80603	14.43757	33.91400	54.58549
6.00	6.09961	15.25574	24.63927	9.50389	22.79976	36.72306	17.30724	40.61021	65.35517
7.00	7.08706	17.66817	28.51364	11.06674	26.49943	42.66927	20.17918	47.31728	76.14349
8.00	8.07770	20.09381	32.41170	12.63195	30.20986	48.63441	23.05255	54.03125	86.94359
9.00	9.07051	22.52867	36.32628	14.19875	33.92766	54.61244	25.92689	60.74986	97.75162
10.00	10.06485	24.97020	40.25280	15.76667	37.65073	60.59966	28.80190	67.47174	108.56521

Table 3 Comparison of the first non-dimensional natural frequency

Hub radius δ	Angular speed	Present result	Reference result (Bogdanoff and Horner)	Discrepancy (%)
0	0.01	1.00005	1.00005	0.000
0	0.10	1.00535	1.00498	0.037
0	1.00	1.43107	1.41421	1.192
1	0.01	1.00014	1.00011	0.003
1	0.10	1.01391	1.01273	0.110
1	1.00	1.90184	1.88733	0.769
5	0.01	1.00049	1.00044	0.005
5	0.10	1.04720	1.04312	0.391
5	1.00	3.09431	3.13209	1.221

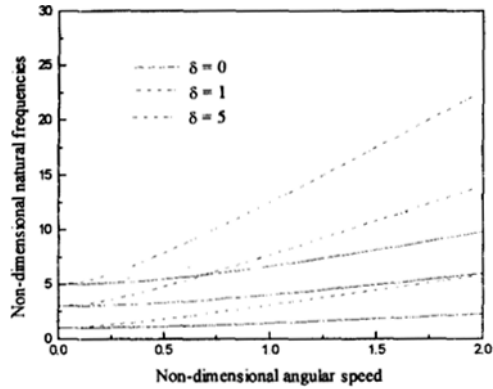


Fig. 2 Natural frequency vs. angular speed

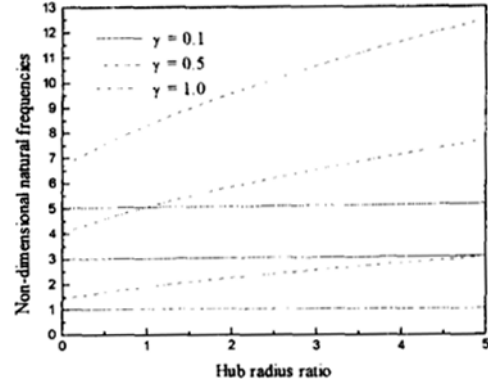


Fig. 3 Natural frequency vs. hub radius ratio

checked by monitoring the difference between results using less modes and those using more modes. Table 1 shows typical results of three lowest natural frequencies for a rotating rod when δ is 1, and γ is 10. As shown in the table, the natural frequencies are converging rapidly as more modes are added. Especially, it is shown that the convergence of the lower modes is faster than the higher modes. Since the results of using 20 modes are only slightly different from those of using 10 modes, all the results shown hereafter were obtained by using 10 modes.

Table 2 displays the lowest three non-dimensional torsional natural frequencies for various values of two parameters: δ and γ . The table shows that all three non-dimensional torsional natural frequencies increase with γ , which is an intuitively expected result. However, since the fundamental torsional natural frequencies of cantilever rods are usually quite high, the actual variations of natural frequencies are small when rods rotate slowly. For instance, for a rod of fundamental torsional natural frequency of 300 rad/s rotating at 6 rad/s, the variation of the first natural frequency is less than 0.07 rad/s (for $\delta=0$). Even with a quite large hub radius (for $\delta=5$), the frequency increase is less than 0.6 rad/s. This small frequency variation might be important only for very accurate design of mechanical systems. Variations of natural frequencies, however, become quite large when rods rotate fast. For instance, if the same rod (introduced above) rotates with an angular speed of 150 rad/s, the

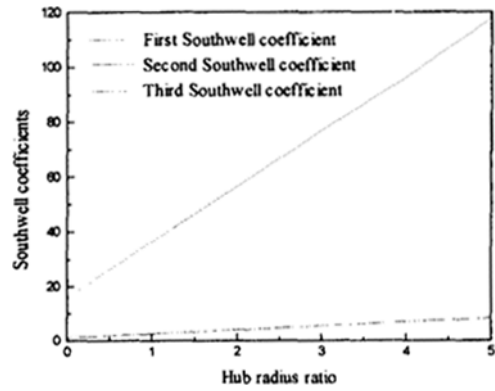


Fig. 4 Southwell coefficients vs. hub radius ratio

variation of its first natural frequency is about 37.5 rad/s. Thus, the first natural frequency of the rotating rod becomes approximately 337.5 rad/s. The variations of the second and third natural frequencies are even larger than that of the first natural frequency. The second and third natural frequencies are originally 900 rad/s and 1500 rad/s when the rod does not rotate. They become approximately 989 rad/s and 1645 rad/s when the rod rotates with an angular speed of 150 rad/s. Thus, the variations are 89 rad/s and 145 rad/s, respectively. It should be noted, however, that the relative increase ratios (the ratios of the variations to the non-rotating natural frequencies) of the second and third natural frequencies are slightly smaller than that of the first natural frequency. Table 2 also shows that the increase in natural frequencies due to rotation is larger when δ increases. This result is also expected: as the

hub radius becomes larger, the centrifugal force becomes larger, and thus, the stiffening effect induced by the centrifugal force increases.

To complement the information in Table 2, Figs. 2 and 3 display the variation of the natural frequencies versus system parameters. In Fig. 2, the lowest three frequencies are plotted versus γ . Three cases of hub radius ratio are shown in the figure. The solid line is for $\delta=0$, the dotted line for $\delta=1$, and the broken solid line for $\delta=5$. The figure clearly shows that natural frequencies increase with the angular speed and that increase ratio becomes higher for larger hub radius. In Fig. 3, the natural frequencies are plotted versus δ , the ratio of the hub radius to the rod length, for three values of angular speed ratios: solid lines are for $\gamma=0.1$, dotted lines for $\gamma=0.5$, and broken solid lines for $\gamma=1.0$. Figure 3 shows clearly that the torsional natural frequencies change very little when γ is small as δ increases. For instance, solid lines look nearly flat in the figure. However, for larger γ , the natural frequencies change more rapidly. Therefore the stiffening effect due to the increase of the hub radius on the natural frequencies of a rotating rod becomes significant only when the angular speed is relatively high.

The results presented in this paper are compared to other results for the accuracy confirmation. Table 3 presents the first natural frequency of the rotating cantilever rod with three different hub radius ratios (δ) and varying angular speed ratios (γ). The results by the present approach and those by Ref. (Bogdanoff and Horner, 1956) are compared in the table. The comparison shows reasonable agreement (maximum difference of 1.2%) between the two results.

Figure 4 shows the variations of first three lowest Southwell coefficients (vs. the hub radius ratio δ) obtained by the eigenvalue problem of Eq. (66). The variations of the Southwell coefficients look almost like straight lines. Table 4 compares the results obtained by the present approach to those by Ref. (Bogdanoff and Horner, 1956). In Ref. (Bogdanoff and Horner, 1956), the Southwell coefficient of the first torsional

natural frequency is given as a linear function of the hub radius ratio. The table shows that the discrepancy between the two results increases as the hub radius ratio increases.

The effect of rotation on the torsional mode shapes is another important subject. Mode shape information is often used in the design of mechanical systems. For example, knowledge of the locations of the nodes (the zero displacement points) are of great importance in the control of mechanical systems. Figure 5 shows the variation of the lowest three mode shapes of the rod in torsion. Solid lines represent the mode shapes of the non-rotating rod and dotted lines are for the rotating rod with $\gamma=10$ (in both cases $\delta=1$). One can observe that the nodal points move toward the free end of the rod when the rod rotates.

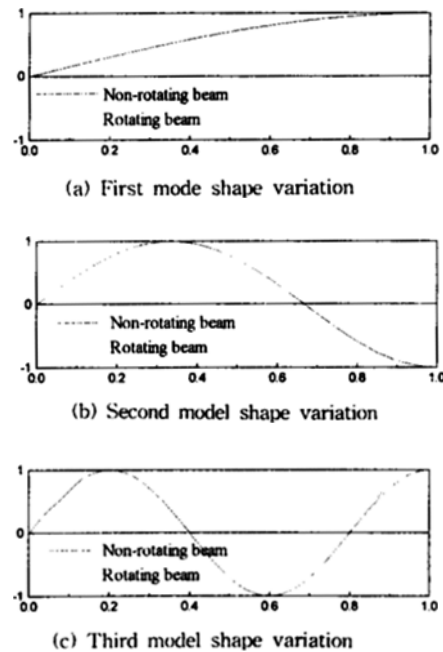


Fig. 5 Variation of mode shapes (non-rotating beam vs. rotating beam)

Table 4 Comparison of the southwell coefficients for the first natural frequency

Hub radius δ	Present result	Reference result (Bogdanoff and Horner)	Discrepancy (%)
0.0	1.001	1.000	0.10
0.5	1.742	1.781	2.19
1.0	2.473	2.562	3.47
1.5	3.201	3.343	4.25
2.0	3.928	4.124	4.75
2.5	4.654	4.905	5.12
3.0	5.380	5.686	5.38
3.5	6.101	6.467	5.66
4.0	6.831	7.248	5.75
4.5	7.556	8.029	5.89
5.0	8.281	8.810	6.00

6. Conclusions

A simple and consistent formulation for deriving the linear equations of motion governing the torsional vibrations of rotating rods is presented in this paper. The formulation eliminates unnecessary, complicated, and perhaps inconsistent steps involved in the conventional method. The key step of this formulation is the introduction of a quadratic strain energy form, expressed in a non-Cartesian deformation variable, which includes the elastic coupling between the axial tension and the torsion of rods, and thus enables the presented formulation to accurately predict torsional natural frequencies and mode shapes of rotating rods. Two non-dimensional parameters are identified through a dimensional analysis: the ratio of the angular speed of the rigid hub to the fundamental torsional natural frequency of the non-rotating rod, and the ratio of the hub radius to the rod length. It is shown that the non-dimensional natural frequencies increase with the angular speed, and the increase rate becomes higher as the hub radius ratio increases. The eigenvalue problem was modified to derive another eigenvalue problem from which one can obtain the Southwell coefficients. The results obtained by the present approach are in good agreement with some existing results. It is also shown that mode

shapes change significantly when rods rotate. Specifically, nodal points move farther from the center of rotation when the rotation speed increases. Lastly, it should be emphasized that the present work claims by no means solutions for general problems. The method presented in this work is restricted to rods with cross sections of high thickness ratio. However, the significance of general cross section shape as well as the warping effect can be investigated with a reference such as the one presented in this paper.

References

- Berdichevskii, V., 1981, "On the Energy of an Elastic Rod," *Prikl. Matem. Mekhan.* Vol. 45, No. 4, pp. 704~718.
- Biot, M. A., 1939, "Increase of Torsional Stiffness of a Prismatical Bar Due to Axial Tension," *Journal of Applied Physics*, Vol. 10, No. 12, pp. 860~864.
- Borri, M. and Mantegazza, P., 1985, "Some Contributions on Structural and Dynamic Modeling of Rotor Blades," *L'Aerotecnica Missili e Spazio*, Vol. 64, No. 9, pp. 143~154.
- Borri, M. and Merlini, T., 1986, "A Large Displacement Formulation for Anisotropic Beam Analysis," *Mechanica*, Vol. 21, pp. 30~37.
- Bogdanoff, J. and Horner J., 1956, "Torsional Vibrations of Rotating Twisted Bars," *J. Aero-*

naut. Sci., Vol. 23, pp. 393~395.

Budiansky, B. and Mayers, J., 1956, "Influence of Aerodynamic Heating on the Effective Torsional Stiffness of Thin Wings," *Journal of the Aeronautical Sciences*, Vol. 23, No. 12, pp. 1081~1093.

Carnegie, W., 1959, "Vibrations of Pretwisted Cantilever Blading," *Proceedings of the Institution of Mechanical Engineers*, Vol. 173, No. 12, pp. 343~374.

Carnegie, W., 1962, "Vibrations of Pre-Twisted Cantilever Blading: An Additional Effect Due to Torsion," *Proceedings of the Institution of Mechanical Engineers*, Vol. 176, No. 13, pp. 315~322.

Chu, C., 1952, "The Effect of Initial Twist on the Torsional Rigidity of Thin Prismatical Bars and Tubular Members," *Proceedings of the First U. S. National Congress of Applied Mechanics*, E. Sternberg, ed., ASME, New York, pp. 265~269.

Danielson, D. and Hodges, D., 1987, "Non-linear Beam Kinematics by Decomposition of the Rotating Tensors," *Journal of Applied Mechanics*, Vol. 54, No. 2, pp. 258~262.

Duggan, A. P., and Slyper, H. A., 1969, "Torsional Vibration of Pretwisted Cantilever Beams," *International Journal of Mechanical Sciences*, Vol. 11, pp. 871~883.

Goodier, J. N., 1950, "Elastic Torsion in the Presence of Initial Axial Stress," *ASME Journal of Applied Mechanics*, Vol. 17, pp. 383~387.

Hodges, D., 1989, "A Mixed Variational Formulation Based on Exact Intrinsic Equations for Dynamics of Moving Beams," *Proceedings of the American Helicopter Society National Specialists' Meeting on Rotorcraft Dynamics*, Arlington, Texas.

Hodges, D. H. and Dowell, E. H., 1974, "Non-linear Equations of Motion for the Elastic Bend-

ing and Torsion of Twisted Nonuniform Blades," NASA TN D-7818.

Houbolt, J.C. and Brooks, G. W., 1958, "Differential Equations of Motion for Combined Flapwise Bending, Chordwise Bending, and Torsion of Twisted Nonuniform Rotor Blades," NACA TR-1346.

Kane T. R. and Levinson, D. A., 1985, *Dynamics: Theory and Applications*, McGraw-Hill Book Company, New York.

Kaza, K. R. V. and Kvaternik, R. G., 1977, "Nonlinear Aeroelastic Equations for Combined Flapwise Bending, Chordwise Bending, Torsion and Extension of Twisted Nonuniform Rotor Blades in Forward Flight," NASA TM-74059.

Kaza, K. R. V. and Kielb, R. E., 1984, "Effect of Warping and Pretwist on Torsional Vibrations of Rotating Beams," *ASME Journal of Applied Mechanics*, Vol. 51, pp. 913~920.

Meirovitch, L., 1980, *Computational Methods in Structural Dynamics*, Sijthoff & Noordhoff, Maryland.

Niedenfuhr, F. W., 1955, "On the Possibility of Aeroelastic Reversal of Propeller Blades," *Journal of the Aeronautical Sciences*, Vol. 22, No. 6, pp. 438~440.

Shield, R., 1984, "A Consistent Theory for Elastic Deformations with Small Strains," *Journal of Applied Mechanics*, Vol. 51, pp. 717~723.

Subrahmanyam, K. B. and Kaza, K. R. V., 1985, "Finite Difference Analysis of Torsional Vibrations of Pretwisted, Rotating, Cantilever Beams with Effects of Warping," *Journal of Sound and Vibration*, Vol. 99 (2), pp. 213~224.

Wagner, H., 1936, "Torsion and Buckling of Open Sections," NACA TM-807.

Wempner, G., 1973, *Mechanics of Solids with Applications to Thin Bodies*, McGraw-Hill Book Company, New York.